J. Membrane Biol. 195, 1–8 (2003)
DOI: 10.1007/s00232-003-2036-6

The Journal of
Membrane
Biology

The Human Red Cell Voltage-regulated Cation Channel. The Interplay with the Chloride Conductance, the Ca^{2+}-activated K^+ Channel and the Ca^{2+} Pump

P. Bennekou[1], **B.I. Kristensen**[1], **P. Christophersen**[2]
[1]The August Krogh Institute, University of Copenhagen, Universitetsparken 13, 2100 Copenhagen, Denmark
[2]NeuroSearch A/S, Pederstrupvej 93, 2750 Ballerup, Denmark

Received: 16 December 2002/Revised: 14 April 2003

Abstract. The activation/deactivation kinetics of the human erythrocyte voltage-dependent cation channel was characterized at the single-channel level using inside-out patches. It was found that the time dependence for voltage activation after steps to positive membrane potentials was slow ($t_{1/2}$ about 30 s), whereas the deactivation was fast ($t_{1/2}$ about 15 ms). Both activation and deactivation of this channel were also demonstrated in intact red cells in suspension. At very positive membrane potentials generated by suspension in extracellular low Cl^- concentrations, the cation conductance switched on with a time constant of about 2 min. Deactivation of the cation channel was clearly demonstrated during transient activation of the Gárdos channel elicited by Ca^{2+} influx via the cation channel and ensuing efflux via the Ca^{2+} pump. Thus, the voltage-dependent cation channel, the Gárdos channel and the Ca^{2+} pump constitute a coupled feedback-regulated system that may become operative under physiological conditions.

Key words: Erythrocyte — Gárdos channel — Non-selective cation channel — Hysteresis

Introduction

When red cells are suspended in depolarizing media, an increase in the passive fluxes of K^+ and Na^+ is observed [9, 10, 23]. It has furthermore been shown that addition of Ca^{2+} to the suspension under these conditions could lead to an activation of the Ca^{2+}-activated K^+ channel, the Gárdos channel [16].

Halperin et al. [15], using the CCCP-method to estimate the membrane potential, proposed that the salt leak in solutions of low ionic strength was caused by an ion channel activated at potentials more positive than 40 mV [16]. In single-channel experiments on excised human red cell inside-out patches, the presence of a non-selective voltage-dependent cation channel (NSVDC channel) with equal conductances for K^+ and Na^+ was demonstrated [8]. It has furthermore been shown that the channel is permeable to Ca^{2+}, Mg^{2+} and Ba^{2+} [21]. Although the definitive proof for the identity of the NSVDC channel with the pathway activated when cells are suspended in depolarizing Ringers is missing, the properties shared by the two systems seem convincing as circumstantial evidence.

In the human red cell the NSVDC channel is believed to be effectively closed at the normal membrane potential of −12 mV. Furthermore, due to the low Ca^{2+} permeability and the large Ca^{2+}-pumping capacity of the erythrocyte membrane, combined with the lack of membrane-delimited intracellular stores that could be released, the Gárdos channel, too, is thought to remain effectively closed. However, these two channels and the Ca^{2+} pump represent in principle a coupled, feedback-regulated system. In the present paper we show that this system becomes operative under depolarizing conditions.

Materials, Methods and Calculations

Reagents

CCCP (Carbonylcyanide-m-chloro-phenyl-hydrazone) and DIDS (4,4′-di-isothiocyanostilbene-2,2′-disulphonate) (Sigma) and NS1652 (2-(N′-trifluoromethylphenyl)ureido)benzoic acid) (synthesized at NeuroSearch (14)) were prepared as stock solutions in DMSO. Salts and sucrose (Sigma) for the Ringers were of analytical grade or better.

Correspondence to: P. Bennekou, email: pbennekou@aki.ku.dk

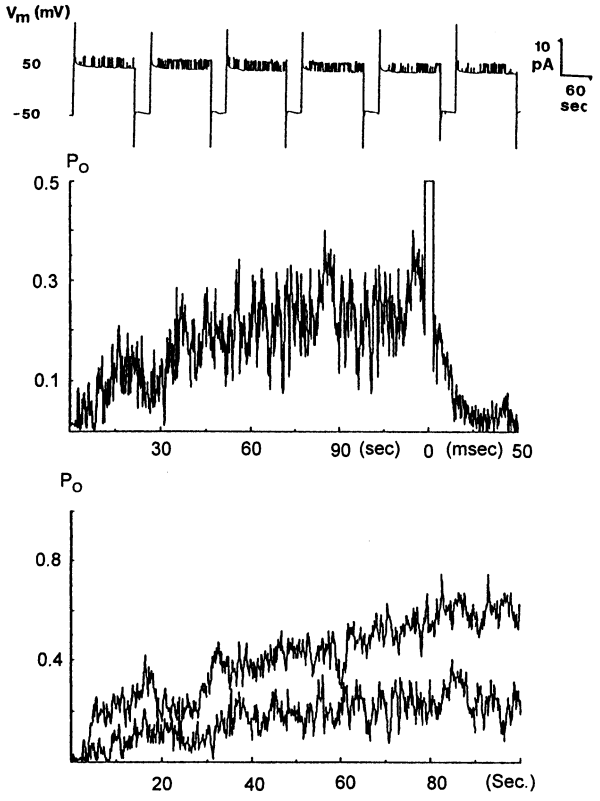

Fig. 1. Time dependence for voltage activation or deactivation of the cation channel. *Upper panel*: The holding potential was alternately switched between 50 mV and −50 mV (32 cycles). The peaks seen when the potential is switched are capacitive transients. A series of six consecutive traces is shown in the figure. Filter cutoff frequency: ~1 kHz. *Middle panel*: The calculated open-state probability from the above experiment as function of time after membrane-potential steps. The calculation was based on the ensemble average current from all cycles. Note the change of time scale to ms in the second part of the curve. *Lower panel*: Comparison of channel activation after steps to 50 mV (same experiment as above) and 100 mV, respectively. The inside-out patch is bathed in symmetric 300 mM KCl solution, in the presence of 50 μM EGTA, pH = 7.4.

Patch Clamp

The patch-clamp experiments were performed as previously described [8].

Red Cell Suspensions

Packed cells were injected into the test solutions and membrane potential and Na^+ and K^+ efflux determined as previously described [3]. Irreversible DIDS inhibition: Cells (10% htc.) were incubated in a 90 mM KCl, 66 mM NaCl solution with 10 μM DIDS at 38°C for 30 minutes, washed three times with unbuffered saline and stored on ice as packed cells.

Membrane Current Estimation

The change in extracellular potassium concentration has a sigmoid shape and can phenomenologically be fitted to a Hill-type equation of the form:

$$[K^+]_{ex}(t) = K_0 + \frac{K_1 \cdot K_3 \cdot t^{K_2}}{1 + K_3 \cdot t^{K_2}} \quad (1)$$

The net flux at a given time is calculated from the time derivative of the fitted curve times a constant depending on the hematocrit.

The Driving Force—Nernst Potentials

Salt loss causes the cells to shrink, but due to the non-ideal osmotic effect of hemoglobin, the water loss does not fully compensate for the salt loss [14], a discrepancy that increases as the hemoglobin becomes more concentrated. Consequently, the molarity of the intracellular salt decreases concomitant with an increase in the extracellular concentration, causing a decrease with time of the Nernst potentials. A model has previously been published [2] from which changes in intracellular concentrations of K^+ and Cl^- as a function of the KCl loss were estimated. As standard initial values, intracellular concentrations of K^+ = 140 mM, Na^+ = 15 mM, Hb = 7.3 mmolal and a cellular water fraction of 0.7 were used. $[Cl]_{cell}$ was calculated from the membrane potential measured in 156 mM Cl^-.

Conductances

The relation between the membrane current i_i of a given ion and the driving force can be expressed as $i_i = g_i (V_m - E_i)$ [18], where g_i, the conductance, is a phenomenological function.

The total membrane current, I_m, due to the passive, electrogenic pathways, which is the sum of all the ion currents, is given by:

$$I_m = \sum_{i=1}^{n} i_i = C_m \frac{dV_m}{dt} + \sum_{i=1}^{n} g_i (V_m - E_i) = 0 \quad (2)$$

where n is the number of individual, discernible conductive pathways, i_i the individual ion current, C_m the membrane capacitance, V_m the membrane potential, and g_i and E_i the conductances and equilibrium potentials. For cells dominated by the passive K^+, Na^+ and Cl^- currents, and provided $dV_m/dt = 0$, the cation conductance can be expressed as:

$$\left(g_{K^+} + g_{Na^+} \frac{V_m - E_{Na^+}}{V_m - E_{K^+}}\right) = g_+ = g_{Cl} \frac{E_{Cl} - V_m}{V_m - E_{K^+}} \quad (3)$$

Results

Application of positive potentials (>30 mV) to a human red cell inside-out patch incorporating a voltage-dependent, nonselective channel results in activation of the channel, which is evident from opening events that become more frequent with time. Upon switching the potential to negative potentials the channel deactivates fast. To elucidate this time-dependent behavior, a sequence of repeated, identical experiments was performed and subsequently summed, in which the potential was switched repeatedly between −50 mV for 30 s (deactivation) and varied positive potentials for 120 s (activation). Fig. 1, *upper panel*, shows the current traces (raw data), from six consecutive cycles (−50 mV and 50 mV). To estimate the relaxation time constants for activation and deactivation, all current traces obtained at the same

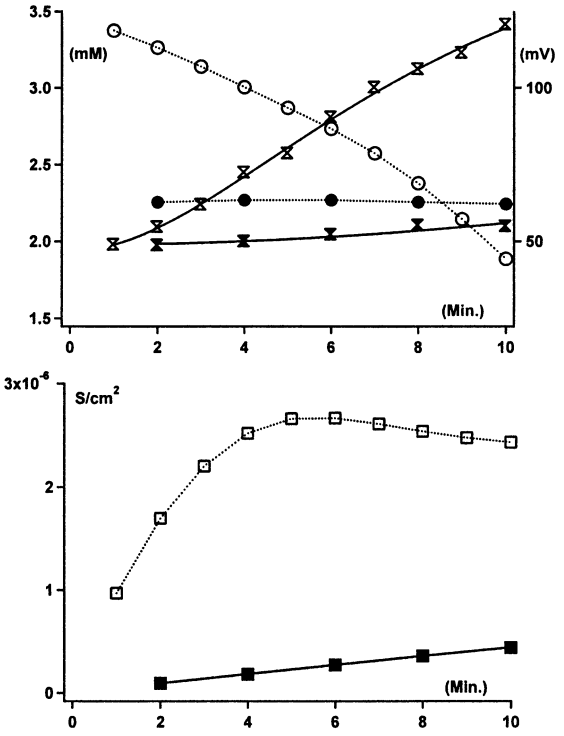

Fig. 2. Membrane potential, extracellular K^+ concentration and cation conductance as function of time for red cells injected into sucrose-substituted Ringer's solution. Closed symbols: 10 mM Cl^-, open symbols: 1 mM Cl^-. *Upper panel*: Changes in membrane potential (right ordinate axis, *dashed lines*) and extracellular K^+ concentration (left ordinate axis, *unbroken lines*). Initially the membrane potential attains a value corresponding to the Nernst potential for chloride. For salt concentrations below 10 mM, however, the membrane potential becomes less positive with time, partly due to opening of the NSVDC channel (the Nernst potentials for the cations K^+ and Na^+ are initially about −110 mV) and partly due to degradation of the ion gradients. *Lower panel*: Potassium conductances (ordinate axis, Siemens/cm^2), corresponding to the potential traces and K^+ efflux shown in the upper panel. The conductances are calculated from net efflux of potassium, as described in the section on Methods.

potential were added and divided by the number of cycles to give an ensemble average current as a function of time. In Fig. 1 (*middle panel*) the corresponding change in open-state probability at +50/−50 mV cycles is shown. Upon activation the open-state probability increased nearly exponentially from 0 to a steady-state value of 0.25 with an estimated time constant of about 30 s. Deactivation was orders of magnitude faster with a time constant around 15 ms. Figure 1 (*lower panel*) shows time-dependent open-state probabilities from cycles with activating potentials of +50 and +100 mV, respectively. The final open-state probability obtained at 100 mV (approximately 0.7) is higher than that at +50 mV, whereas the time constant was not appreciably changed.

The activation/deactivation behavior of the NSVDC channel was reflected by intact red cells in suspension. The delayed activation part was clearly seen when erythrocytes were suspended in unbuffered Ringer solution with low concentrations of permeable anions. Due to the dominating red cell Cl^- conductance, V_m was initially clamped at the positive E_{Cl}. Depending on the degree of anion substitution, either a stable Cl^--clamped positive potential ensued (156 mM > $[Cl^-]_o$ > 10 mM) or the membrane potential began to drift away from E_{Cl} in the negative direction (10 mM > $[Cl^-]_o$ > 0 mM) with a concomitant initiation of salt efflux. As seen from Fig. 2, (*upper panel*) the plot of the extracellular K^+ concentration *vs.* time is markedly sigmoid under these conditions and consistently well fitted by Eq. 2, the derivative of which is proportional to the net efflux. The change in membrane potential reflects partly the increased cation conductance due to activation of the NSVDC channels and partly the concomitant dissipation of the concentration gradients over time. Based on the membrane potential, the net efflux and the Nernst potential for K^+, the time course of the K^+ conductance was calculated.

Figure 2 (*lower panel*) shows that the voltage-induced cation conductance increase at Cl^- substitutions below 2 mM, resulting in very positive potentials, reached a maximum of about 3 μS/cm^2 after 6 to 8 minutes. At lower degrees of substitution, corresponding to less positive initial membrane potentials, the conductance increase did not saturate after 20 minutes.

It should be noted, that induction of the cation conductance is due to the depolarization per se and not the low ionic strength in sucrose Ringer's, since identical results are obtained with red cells injected into Ringer's containing impermeable anions, such as gluconate. Furthermore, the cation conductance is independent of the presence of intracellular chloride, since cells where chloride is exchanged with nitrate show comparable increase in conductance, up to about 3 μS/cm^2 in full-sucrose Ringer.

The deactivation part of the voltage-dependent cation-channel kinetics can be demonstrated by inducing a strong, deactivating hyperpolarization by an ensuing activation of the Gárdos channel. In order to avoid pronounced dissipation of the ion gradients and to maximize the hyperpolarizations, these experiments were performed with blocked anion conductance, either in the presence of the reversible inhibitor, NS1652, [7] or on cells pre-incubated with DIDS, resulting in irreversible inhibition. Rather than activating the Gárdos channel with the Ca^{2+} ionophore, A23187, we took advantage of the sizeable Ca^{2+} permeability of the activated voltage-dependent cation channel in order to obtain the necessary Ca^{2+} influx.

Figure 3 shows the membrane potential changes after injection of cells into 2 mM Cl^--solutions containing 10 μM NS1652. With an estimated residual

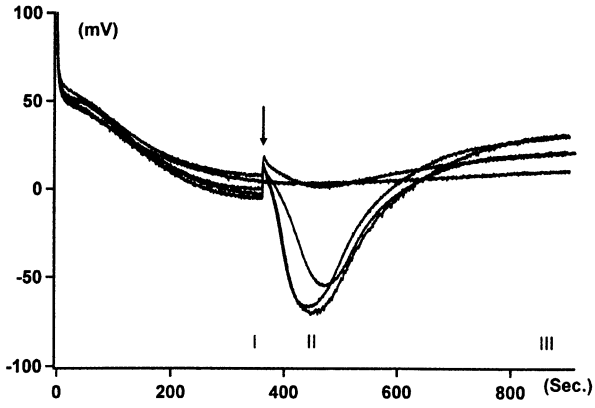

Fig. 3. Calcium dose-response. The trace shows the membrane potential estimated from CCCP-mediated changes in extracellular pH. Arrow indicates Ca^{2+} addition as 1 M stock solution of calciumgluconate. Final concentrations 0, 0.5, 1, 1.5 and 2 mM. Increasing hyperpolarizations are attained with increasing Ca^{2+} concentration. Roman numerals indicate 3 phases in the experiments: I, the stationary state attained in sucrose Ringer; II, the peak hyperpolarization after addition of Ca^{2+}; and III, the stationary state following closing of the Ca^{2+}-activated K^+-channel.

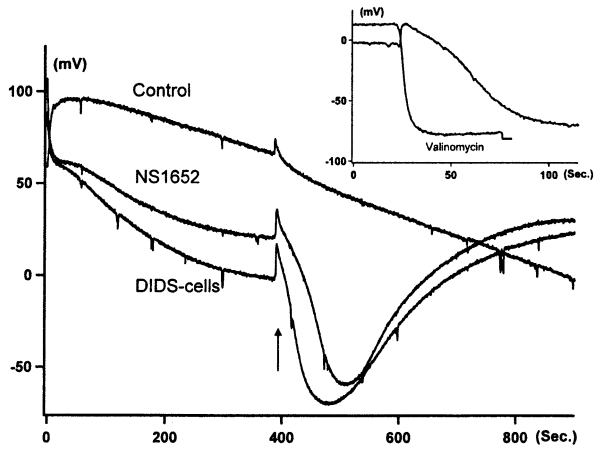

Fig. 4. Chloride conductance block and Ca^{2+} challenge. The figure shows the development with time of the membrane potential after the cells have been suspended in a sucrose Ringer (2 mM KCl, sucrose to isotonicity). The initial chloride Nernst potential is about 106 mV. It is seen that the unblocked cells (*control*) attain an initial membrane potential very close to this value, which then changes slowly over time. The blocked cells, (NS1652 and DIDS) initially change the membrane potential very fast, since the potential-induced change in cation conductance has a higher weight in the high-impedance system. Although the calcium-induced potential peak is absent in the unblocked experiment, the rate of the potential change is higher after Ca^{2+} addition. Arrow indicates addition of calciumgluconate to a final concentration of 2 mM. *Insert*: Potential changes (ordinate axis) estimated from the CCCP-mediated changes in extracellular pH after valinomycin addition (final concentration $5 \cdot 10^{-7}$ M) and Ca^{2+} addition (2 mM) *vs.* time.

Cl^--conductance of about 10%, the membrane potentials reproducibly attain less positive values and drift faster in the hyperpolarizing direction in comparison to the control experiments without blocked Cl^- conductance (*see* Fig. 2). When a stationary potential of approximately 0 mV was reached after 6.5 min, Ca^{2+} (as gluconate salt) was added to a final concentration of 0, 0.5, 1.0, 1.5 or 2.0 mM, respectively. Above a threshold of about 0.5 mM, the Ca^{2+} additions dose-dependently elicited hyperpolarizations becoming faster and more pronounced with increasing Ca^{2+} concentration, reaching values of about -70 mV. It should be noted that the transient responses genuinely reflect the time course of the potential change, since the CCCP system can report valinomycin-induced changes in membrane potential as fast as -19 mV/s (*see* Fig. 3, insert), whereas the maximum change after addition of Ca^{2+} is only about -2 mV/s. The hyperpolarizing responses were transient in nature with the ensuing depolarization initiated by closure of the Gárdos channel, due to Ca^{2+} extrusion by the Ca^{2+} pump. However, since the *post*-hyperpolarization membrane potentials stabilized at more positive values than *pre*-hyperpolarization values, deactivation of the voltage-dependent cation channel must have occurred, too.

These observations have been quantified in the experiments illustrated in Figs. 4 and 5. Figure 4 shows the membrane potential recordings from 3 experiments (unblocked Cl^- conductance; NS1652 reversibly blocked Cl^- conductance, DIDS irreversibly blocked Cl^- conductance) performed as described in Fig. 3. As expected, the initial drift away from E_{Cl} caused by activation of the voltage-dependent channel as well as the Ca^{2+}-induced hyperpolarization caused by the Gárdos channel activation was slightly more pronounced with DIDS-treated cells (residual Cl^- conductance about 1 $\mu S/cm^2$) than with NS1652 (residual Cl^- conductance about 2.5 $\mu S/cm^2$). Figure 5 shows the corresponding changes in extracellular K^+ (*upper panel*) and conductances (*lower panel*). For the control experiment, the K^+ conductance has attained the relatively high level of 1 $\mu S/cm^2$ after 1 min. It increases with time to about 3 $\mu S/cm^2$; with only little effect from the addition of Ca^{2+}, probably due to the very small driving force on the Ca ion at this potential. In the case of cells with blocked chloride conductance, the initial conductances for K^+ are about 0.1 (NS1652) and 0.4 (DIDS) $\mu S/cm^2$, increasing to 1.0 and 0.7 $\mu S/cm^2$, respectively, immediately before the addition of Ca^{2+}. After addition of Ca^{2+}, peak conductances of about 3 and 2 $\mu S/cm^2$ are reached, followed by a decrease to about 0.4 and 0.5 $\mu S/cm^2$, confirming the deactivation of the voltage-gated cation channel.

The initial depolarization is enhanced if the cells are suspended in a sucrose Ringer without cations, compared to the experiments with 1 or 2 mM salt present, but a transient calcium-induced hyperpolarization cannot be triggered, *see* Fig. 6, upper panel. It is, however, not the absence of salt per se that pre-

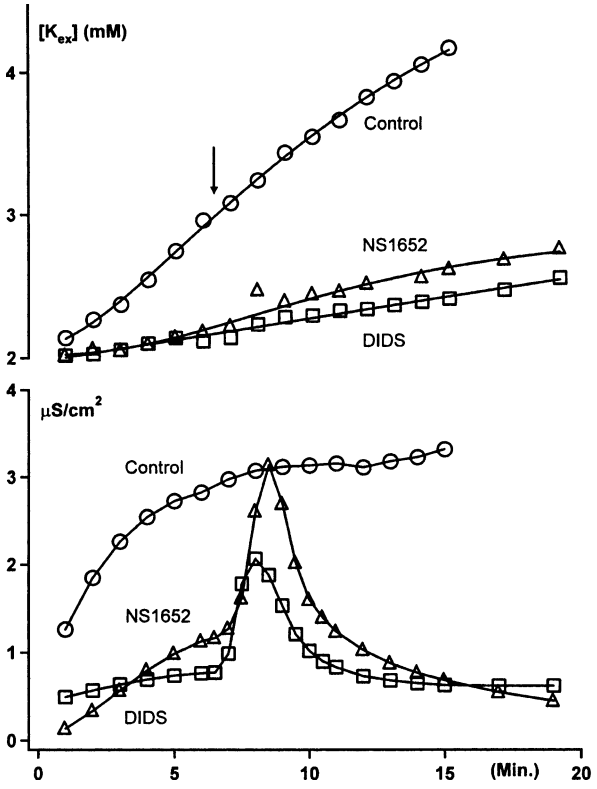

Fig. 5. Extracellular K^+ concentration (*upper panel*): and cation conductance (*lower panel*): as function of time corresponding to the potential traces shown in Fig. 3.

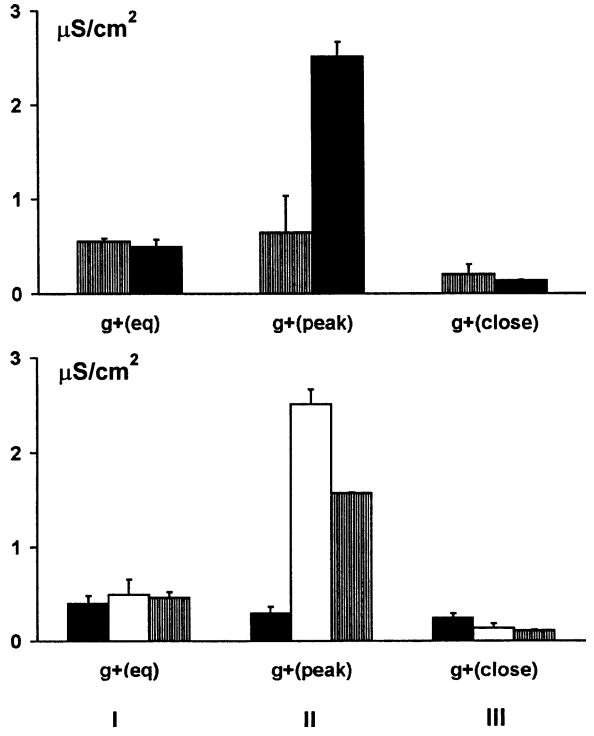

Fig. 6. *Upper panel*: The calcium response in dependence of 0 (*gray columns*) or 1 (*solid columns*) mM K^+ in the extracellular medium. In the absence of K^+, no hyperpolarization is observed after addition of Ca^{2+}. *Lower panel*: Dependence on the species of cation present in the extracellular solution. No response is seen when the only cation present in the extracellular solution is 1 mM sodium (*black columns*). In the presence of 1 mM rubidium (*gray columns*), a hyperpolarization peak is observed, which is smaller than the peak observed in the presence of 1 mM potassium (*white columns*). Roman numerals corresponding to Fig. 3 indicate the time at which the conductances have been calculated.

vents the release of the Ca^{2+} response, but the species of cation present in the extracellular solution. If the only cation ion present in the sucrose Ringer is sodium (1 mM) no response to the Ca^{2+} addition is seen, while in the presence of rubidium (1 mM) a hyperpolarization peak is observed, which, however, is less negative than the peak observed in the presence of potassium, Fig. 6, lower panel.

Discussion

Single-channel experiments show that the rate of activation of the NSVDC channel is slow compared to the deactivation, with a half time, $t_{1/2}$, for activation of about 30 s and a $t_{1/2}$ for deactivation of about 15 ms, when the holding potential is switched between ± 50 mV, giving an on/off ratio of about 1/2000. Activating potentials of +100 mV gave comparable results. However, as can be seen from the summed traces, Fig. 1, middle and lower panels, the fluctuations, using 32 cycles, are still too dominating to make a determination of mono/multi-exponentiality or rate constants possible. It should be noted that 32 cycles correspond to a duration of a single experiment of 80 minutes, which is long compared to the mean life time of a patch. This line of investigation was consequently not pursued further.

It has previously been reported that the voltage activation of the NSVDC channel has hysteresis-like properties [6, 21] with an upper and a lower leg, depending on the polarity of the initial holding potential. The estimated equilibrium open-state probability is about 0.25 at +50 mV in the present experiment, which is consistent with an activation along the lower leg in accordance with activation from negative potentials.

However, to what extent is this and previously published results from single-channel experiments reflected in the behavior of intact red cells? Experimentally, the control over the holding potentials and over the composition of the bathing solutions, which is possible for an inside-out patch is not attainable with intact cells in suspension. Under the present experimental conditions the response observed was the contribution from 10^9 cells (100 μl packed cells), with an estimated number of $3 \cdot 10^{11}$ NSVDC channels [4], and with the cell machinery intact. Further-

more, injection of packed cells into a substituted Ringer does not lead to a perfect synchronization of the cells compared to the instantaneous shift of a holding potential.

It is well known that human red cells when suspended in Ringer's that causes a depolarization, respond with an increase in the conductance of the cations. Apart from the conductive pathways, evidence has been presented for the participation of a $K^+(Na^+)/H^+$-exchanger in the salt loss from red cells suspended in low ionic-strength Ringer's [22, 24]. However, with regard to the results reported here, nearly identical results are obtained for the cation conductances, whether calculated from the K^+ loss representing the K^+ current, i_K, and the driving force or from Eq. 3 and a separate determination of the chloride conductance in valinomycin experiments. Consequently, should an exchange mechanism be operative, it is only of minor importance under the present experimental conditions.

Under physiological conditions the normal human red cell has a high conductance for chloride, about 25 $\mu S/cm^2$ [2], and a very low conductance for cations. When the cells are depolarized by suspension in Ringer's solutions where the concentration of permeable anions is below 2 mM, the conductance slowly increases to about 3 $\mu S/cm^2$ (Fig. 1, upper panel). As a consequence, this increase in cation conductance will result in a massive loss of salt. Since the passive transport of cations is dependent on the kinetics for these ions as well as on the counter ions [5], inhibition of the anion pathway by application of inhibitors of chloride conductance limits the net loss of salt.

Cells with the normal high chloride conductance are more effectively clamped to a potential corresponding to the Nernst chloride conductance (*see* Fig. 4) when suspended in depolarizing Ringer's. However, under these conditions the ion gradients are degraded relatively fast, as can be seen from the change in extracellular K^+ concentration, Fig. 5, upper panel. If a chloride conductance blocker is applied, this degradation is retarded, due to a reduction of the g_{Cl} to 1–2.5 $\mu S/cm^2$, but at the cost of a fast changing (hyperpolarizing) membrane potential due to the relatively greater increase in cation conductances. This is apparent from the experiments shown in Figs. 4 and 5, upper panel. Loss of all intracellular Cl^- under the present experimental conditions will result in an extracellular increase in KC1 of about 2.5 mM, which is approached after 15 minutes in the case of unblocked g_{Cl}. For cells with the chloride conductance blocked by 10 μM NS1652, the depolarization is far more pronounced and even more for DIDS-treated cells, having a g_{Cl} of 1 $\mu S/cm^2$ compared to about 2.5 $\mu S/cm^2$ in the former case. A block of about 90% in the presence of 10 μM NS1652 is in accordance with the effect on cells suspended in normal Ringer's in the presence of valinomycin [7]. The loss of salt is, however, only about 20–25% of the control value (Fig. 5, upper panel).

It has been reported by Jones and Knauf [20] that DIDS inhibits the cation pathway causing depolarization, a finding which Halperin et al. [15] were unable to support. In the present work the induced cation conductances found for DIDS-treated cells or for cells in the presence of the chloride conductance blocker NS1652 are consistently lower than for untreated cells, see Fig. 5, lower panel. Although it is tempting to interpret this result as a block of the cation channel per se, it should be noted that the higher the degree of the chloride conductance block, the faster the cells will hyperpolarize. This results either in a lesser degree of activation or causes a deactivation of the channel. This interpretation is in accordance with the single-channel data as well as the observed time dependence of the channel activation in cells suspended in Ringer's with varied extracellular chloride concentration. The effect of the chloride conductance blockers on the channel activation is therefore considered to be indirect.

With regard to the differences in the observed response to the addition of Ca^{2+}, a number of factors come into play, since the Ca^{2+} influx is dependent on the degree of opening of the NSVDC channel, the driving force for Ca^{2+} entry, the chloride conductance and thereby the degree of chloride inhibition.

To our knowledge, the first observation of a Ca^{2+}-induced hyperpolarization (estimated by the CCCP method) associated with a transient increase of K^+ efflux in a low-chloride medium was reported by Adorante and Macey [1]. They ascribed this, however, to a mechanism different from the Ca^{2+}-activated K^+ channel. Halperin et al. [15], also estimating the membrane potential with CCCP, proposed that the salt leak in solutions of low ionic strength was caused by a separate membrane protein, a voltage-dependent cation channel activated at potentials more positive than 40 mV with the conductance increase reaching 1.5 $\mu S/cm^2$ at +50 mV. An important conclusion from these studies was that the increase in voltage-dependent cation permeability included Ca^{2+}: Addition of 1 mM Ca^{2+} to cells depolarized in a Ca^{2+}-free sucrose medium caused a strong hyperpolarization, which could be inhibited by the addition of carbocyanine, a Gárdos channel inhibitor. This result was interpreted as a secondary activation of the Gárdos channel following influx of Ca^{2+} through the voltage-dependent pathway. This perception is in accordance with the findings from single-channel experiments on the NSVDC channel [21], reporting that the channel is permeable to the divalent cations Mg^{2+}, Ca^{2+} and Ba^{2+}. In the present work a similar activation of the Gárdos channel is observed (*see* Figs. 4 and 5, lower panel), but here followed by a depolarization. However, the rate of calcium influx seems to be crucial with regard to ac-

tivation of the Gárdos channel, which in intact cells has a $K_{0.5}$ of about 1 μM Ca^{2+}. No hyperpolarization is observed if calcium is present in the Ringer before the cells are injected, or if Ca^{2+} is added too early, depending on the degree of substitution. It is a common feature for the Gárdos channel and the Ca^{2+}-ATPase that the Ca^{2+} activation is triggered via binding of Ca^{2+} to calmodulin. Basically, the Ca^{2+} pump and the Gárdos channel could thus be expected to show comparable Ca^{2+} sensitivities, with a $K_{0.5}$ of 1 μM corresponding to calmodulin binding in the presence of physiological concentrations of Mg^{2+} [25]. While calmodulin is constitutively bound to the Gárdos channel [12], the Ca^{2+} pump associates with a relatively low rate constant to the calmodulin-calcium complex formed in the cytosol [25,26]. As the dissociation rate constant also is low, it means that once activated, the pump stays activated for a long time. To paraphrase Scharff and Foder [26], the pump is well suited to maintain Ca^{2+} below 10^{-7} M in the unstimulated cell and to allow Ca^{2+} transients up to 10^{-5} during stimulation. If the rate of calcium entry is low, due to insufficient opening of the NSVDC channel, the Ca^{2+} pump will have sufficient time to become activated and succeed in extruding the Ca^{2+} again before the Gárdos channel is activated (or only marginally activated). At a somewhat higher entry rate the Gárdos channel will be activated before calcium is extruded again, and with a sufficiently high entry rate, the pump is overwhelmed. However, once the intracellular Ca^{2+} concentration has increased to a level causing activation of the Gárdos channel, the resulting hyperpolarization will further increase the Ca^{2+} influx due to the increased driving force. The dependence on the presence of K^+ in the extracellular medium, and the ability of Rb^+ to substitute for K^+ [17], is further evidence for the involvement of the Gárdos channel and in accordance with the high calcium conductance found in single-channel experiments. However, compared to work with A23187-induced Ca^{2+} oscillations [27], only a single potential peak was observed routinely in the present experiments.

In contrast to earlier findings [9] and to single-channel experiments [8], Halperin et al. [15] found persisting conductances for Na^+ and K^+ if the cells were repolarized by transfer to a normal Ringer's solution, resulting in a membrane potential of about −10 mV. This is confirmed by the present experiments, where cells in sucrose Ringer after the initial depolarization have been observed to hyperpolarize to stationary negative membrane potentials. It is thus not possible to decide whether the depolarization following the peak in the Gárdos channel-mediated hyperpolarization is due to a switch-off of the Ca^{2+} entry due to closing of the NSVDC channel at these more negative potentials, or to activation of the Ca^{2+} pump sufficient to lower intracellular Ca^{2+} to a level below Gárdos-channel activation or a combination of both. What is evident, however, is that given a sufficient degree of hyperpolarization, the cation conductance found after the hyperpolarization is lower than before. It has previously been shown, that activation of the NSVDC channel shows hysteresis-like properties, the activation at a given potential being lower if the channel is activated from negative potentials than from positive ones. The observed shift in conductance level after a hyperpolarization is consistent with an activation from positive membrane potentials (when the cells are injected into highly substituted Ringer's) followed by closing of the channel during the hyperpolarization and activation from negative potentials to a lower conductance level. This indicates that the voltage activation/deactivation as well as the hysteretic properties are operative in the intact cell. The voltage activation curve, however, seems to be left-shifted in the intact cell compared to the behavior of the channel when observed in an isolated patch.

The identity of the NSVDC channel found in patch-clamp experiments with the pathway activated in cells suspended in substituted Ringer's, is strengthened by the parallels in the time dependence of the activation and the hysteresis-like behavior. With regard to the activation, however, it should be noted, that the highest degree of activation is found in cells with unblocked chloride conductance, as the initial depolarization is more positive and the membrane potential more stable. Even in this case, conductances only reach a level of about 3 $\mu S/cm^2$. With an estimate of 300 channels/cell [4] and a single-channel conductance of 30 pS/channel, this corresponds to a mean single channel open-state probability of about 0.5×10^{-3}, compared to an open-state probability close to 1 found in patch-clamp experiments at comparable potentials.

Recently, a series of papers, using whole-cell patch clamp on human red cells [11, 13, 19] have been published, characterizing cation currents across the red cell membrane. A common characteristic for these experiments is the determination of a very high conductance. Huber et al., [19], find a whole-cell conductance of 7.4×10^{-9} S/cell, corresponding to about 4.2×10^{-3} S/cm^2. With the estimates for channel number and conductance used above, a theoretical maximum conductance is found to be 9×10^{-9} S/cell or 5.1×10^{-3} S/cm^2, which is in remarkable agreement with the value reported from whole-cell experiments. The experiments on suspensions demonstrate that the time-dependent voltage activation and hysteretic properties are present in the intact cell as well. However, the maximum activation is only 1/2000 of the activation estimated from data from excised patches or observed in whole-cell measurements. It is thus tempting to suspect that some intracellular component, which either downregulates

the channel in the intact cell or makes a large fraction inoperative, has been lost in both excised patches and whole-cell patches, and care should be taken when drawing parallels to the intact cell.

The interplay between the non-specific cation channel, the Gárdos channel and the Ca^{2+} pump, which has been demonstrated here under nonphysiological conditions, might be of potential importance for the Ca^{2+} homeostasis and maintenance of the human red cell membrane potential. If the nonspecific channel opens (even rarely), the conductances for mono- and divalent ions increase, Ca^{2+} influx may activate nearby Gárdos channels leading to hyperpolarization and closing of the nonspecific channel, and subsequently the system is restored to the resting state by the extrusion of Ca^{2+}.

Kirsten Abel, Gurli Bengtson and Søren L. Johansen are gratefully acknowledged for their expert assistance.

References

1. Adorante, J.S., Macey, R.I. 1986. Calcium-induced transient potassium efflux in human red blood cells. *Am. J. Physiol.* **250:**C55–C64
2. Bennekou, P. 1984. K^+-valinomycin and chloride conductance of the human red cell membrane. Influence of the membrane protonophore carbonylcyanide m-chlorophenylhydrazone. *Biochim. Biophys. Acta* **776:**1–9
3. Bennekou, P. 1988. Protonophore anion permeability of the human red cell membrane determined in the presence of valinomycin. *J. Membrane Biol.* **102:**225–234
4. Bennekou, P. 1993. The voltage-gated non-selective cation channel from human red cells is sensitive to acetylcholine. *Biochim. Biophys. Acta* **1147:**165–167
5. Bennekou, P. 1999. The feasibility of pharmacological volume control of sickle cells is dependent on the quantization of the transport pathways. A model study. *J. Theor. Biol.* **196:**129–137.
6. Bennekou, P., Christophersen, P. 1992. A human red cell cation channel showing hysteresis like voltage activation/inactivation. *Acta Physiol. Scand.* **146 Sup: 608:**56
7. Bennekou, P., Pedersen, O., Møller, A., Christophersen, P. 2000. Volume control in sickle cells is facilitated by the novel anion conductance inhibitor NS1652. Blood **95:**1842–1849
8. Christophersen, P., Bennekou, P. 1991. Evidence for a voltage-gated, non-selective cation channel in the human red cell membrane. *Biochim. Biophys. Acta* **1065:**103–106
9. Dawson, H. 1939. Studies on the permeability of erythrocytes. VI. The effect of reducing the salt concentration in the medium surrounding the cell. *Biochem. J.* **33:**389–401
10. Donlon, A.J., Rothstein, A. 1969. The cation permeability of erythrocytes in low ionic strength media of various tonicities. *J. Membrane Biol.* **1:**37–52
11. Duranton, C., Huber, S.M., Lang, F. 2002. Oxidation induces a Cl^--dependent cation conductance in human red blood cells. *J. Physiol.* **539:**847–855
12. Fanger, CM, Ghanshani, S, Logsdon, NJ, Rauer, H, Kalman, K, Zhou, J, Beckingham, K, Chandy, KE, Cahalan, MD, Aiyar, J. 1999. Calmodulin mediates calcium-dependent activation of the intermediate conductance KCa channel, IKCa1. *J. Biol. Chem.* **274:**5746–5754
13. Fomenti, A., Rodighiero, S. 2001. Whole-cell and perforated-patch recordings of voltage-dependent outward and inward cation currents in human red blood cells. XIII Meeting of the European Association for Red Cell Research. 72
14. Freedman, J.C., Hoffman, J.F. 1979. Ionic and osmotic equilibria of human red blood cells treated with nystatin. *J. Gen. Physiol.* **74:**157–185
15. Halperin, J.A., Brugnara, C., Tosteson, M.T., Van Ha, T., Tosteson, D.C. 1989. Voltage-activated cation transport in human erythrocytes. *Am. J. Physiol.* **257:**C986–C996
16. Halperin, J.A., Brugnara, C., van Ha, T., Tosteson, D.C. 1990. Voltage-activated cation permeability in high-potassium but no low-potassium red blood cells. *Am. J. Physiol.* **258:**C1169–C1172
17. Heinz, A, Passow, H. 1980. Role of external potassium in the calcium-induced potassium efflux from human red blood cell ghosts. *J. Membr. Biol.* **57(2):**119–131
18. Hodgkin, A.L., Huxley, A.F. 1952. The components of membrane conductance in the giant axon of Loligo. *J. Physiol.* **116:**449–472
19. Huber, S.M., Gamper, N., Lang, F. 2001. Chloride conductance and volume-regulatory nonselective cation conductance in human red blood cell ghosts. *Pfluegers Arch. - Eur. J. Physiol.* **441:**551–558
20. Jones, G.S., Knauf, P.A. 1985. Mechanism of the increase in cation permeability of human erythrocytes in low-chloride media. *J. Gen. Physiol.* **86:**721–738
21. Kaestner, L., Christophersen, P., Bernhardt, I., Bennekou, P. 2001. The non-selective voltage-activated cation channel in the human red blood cell membrane: Reconciliation between two conflicting reports and further characterization. *Bioelectrichemistry* **52:**117–125
22. Kummerow, D., Hamann, J., Browning, J.A., Wilkins, R., Ellory, J.C., Bernhardt, I. 2000. Variations of intracellular pH in human erythrocytes via $K^+(Na^+)/H^+$ exchange under low ionic strength conditions. *J. Membrane Biol.* **176:**207–216
23. LaCelle, P.L., Rothstein, A. 1966. The passive permeability of the red blood cell to cations. *J. Gen. Physiol.* **50:**171–189
24. Richter, S., Hamann, J., Kummerow, D., Bernhardt, I. 1997. The monovalent cation 'leak' transport in human erythrocytes: An electroneutral exchange process. *Biophys. J.* **73:**733–745
25. Scharff, O. 1981. Calmodulin and its role in cellular activation. *Cell Calcium* **2:**1–27
26. Scharff, O., Foder, B. 1982. Rate constants for calmodulin binding to Ca^{2+}-ATPase in erythrocyte membranes. *Biochem. Biophys. Acta* **691:**133–143
27. Vestergaard-Bogind, B., Bennekou, P. 1982. Calcium-induced oscillations in K^+ conductance and membrane potential of human erythrocytes mediated by the ionophore A23187. *Biochim. Biophys. Acta* **688:**37–44